NeuroImage xxx (2010) xxx–xxx

Contents lists available at ScienceDirect

NeuroImage

journal homepage: www.elsevier.com/locate/ynimg

Genome-wide analysis reveals novel genes influencing temporal lobe structure with relevance to neurodegeneration in Alzheimer's disease

Jason L. Stein [a], Xue Hua [a], Jonathan H. Morra [a], Suh Lee [a], Derrek P. Hibar [a], April J. Ho [a], Alex D. Leow [a,b], Arthur W. Toga [a], Jae Hoon Sul [c], Hyun Min Kang [d], Eleazar Eskin [c,e], Andrew J. Saykin [f,g], Li Shen [f], Tatiana Foroud [g], Nathan Pankratz [g], Matthew J. Huentelman [h], David W. Craig [h], Jill D. Gerber [h], April N. Allen [h], Jason J. Corneveaux [h], Dietrich A. Stephan [p], Jennifer Webster [h], Bryan M. DeChairo [i], Steven G. Potkin [j], Clifford R. Jack Jr. [k], Michael W. Weiner [l,m,n,o], Paul M. Thompson [a,*] and the Alzheimer's Disease Neuroimaging Initiative [1]

[a] *Laboratory of Neuro Imaging, Department of Neurology, UCLA School of Medicine, Neuroscience Research Building 225E, 635 Charles Young Drive, Los Angeles, CA 90095-1769, USA*
[b] *University of Illinois School of Medicine, Chicago, IL USA, and Community Psychiatry Associates, Sacramento, CA, USA*
[c] *Department of Computer Science, UCLA, Los Angeles, CA, USA*
[d] *Department of Biostatistics, University of Michigan, Ann Arbor, Michigan, USA*
[e] *Department of Human Genetics, UCLA, Los Angeles, CA, USA*
[f] *Center for Neuroimaging, Department of Radiology and Imaging Sciences, Indiana University School of Medicine, Indianapolis, IN, USA*
[g] *Department of Medical and Molecular Genetics, Indiana University School of Medicine, Indianapolis, IN, USA*
[h] *The Translational Genomics Research Institute, Phoenix, AZ, USA*
[i] *Neuroscience, Molecular Medicine, Pfizer Global R&D, New London, CT, USA*
[j] *Department of Psychiatry and Human Behavior, University of California, Irvine, Irvine, CA, USA*
[k] *Mayo Clinic, Rochester, MN, USA*
[l] *Department of Radiology, UC San Francisco, San Francisco, CA, USA*
[m] *Department of Medicine, UC San Francisco, San Francisco, CA, USA*
[n] *Department of Psychiatry, UC San Francisco, San Francisco, CA, USA*
[o] *Department of Veterans Affairs Medical Center, San Francisco, CA, USA*
[p] *IGNITE Institute for Individualized Health, Fairfax, VA, USA*

ARTICLE INFO

Article history:
Received 22 October 2009
Revised 15 January 2010
Accepted 22 February 2010
Available online xxxx

ABSTRACT

In a genome-wide association study of structural brain degeneration, we mapped the 3D profile of temporal lobe volume differences in 742 brain MRI scans of Alzheimer's disease patients, mildly impaired, and healthy elderly subjects. After searching 546,314 genomic markers, 2 single nucleotide polymorphisms (SNPs) were associated with bilateral temporal lobe volume ($P<5\times10^{-7}$). One SNP, rs10845840, is located in the *GRIN2B* gene which encodes the *N*-methyl-D-aspartate (NMDA) glutamate receptor NR2B subunit. This protein – involved in learning and memory, and excitotoxic cell death – has age-dependent prevalence in the synapse and is already a therapeutic target in Alzheimer's disease. Risk alleles for lower temporal lobe volume at this SNP were significantly over-represented in AD and MCI subjects vs. controls (odds ratio = 1.273; $P=0.039$) and were associated with mini-mental state exam scores (MMSE; $t=-2.114$; $P=0.035$) demonstrating a negative effect on global cognitive function. Voxelwise maps of genetic association of this SNP with regional brain volumes, revealed intense temporal lobe effects (FDR correction at $q=0.05$; critical $P=0.0257$). This study uses large-scale brain mapping for gene discovery with implications for Alzheimer's disease.

Introduction

The quest to identify genes that influence brain integrity or degeneration has been greatly accelerated by large-scale scanning and genotyping of subjects with Alzheimer's disease (AD) and those at risk with amnestic mild cognitive impairment (MCI). Here we developed a high-resolution mapping approach to associate 546,314 genomic markers with regional volumetric differences in the brain MRI scans of

* Corresponding author. Fax: +1 310 206 5518.
E-mail address: thompson@loni.ucla.edu (P.M. Thompson).
[1] Data used in the preparation of this article were obtained from the Alzheimer's Disease Neuroimaging Initiative (ADNI) database (www.loni.ucla.edu/ADNI). As such, the investigators within the ADNI contributed to the design and implementation of ADNI and/or provided data but did not participate in analysis or writing of this report. ADNI investigators include (complete listing available at http://www.loni.ucla.edu/ADNI/Collaboration/ADNI_Manuscript_Citations.pdf).

1053-8119/$ – see front matter © 2010 Elsevier Inc. All rights reserved.
doi:10.1016/j.neuroimage.2010.02.068

742 subjects. The resulting study is the largest brain mapping to date that has used genome-wide scans, which we applied to create point-by-point maps of genetic association. We found that lower temporal lobe volumes were most associated with a common variant in the glutamate receptor gene, *GRIN2B*. In addition, this risk allele was statistically over-represented in AD and MCI vs. elderly control subjects.

Structural brain degeneration is a characteristic of AD and MCI (Du et al., 2001; Apostolova et al., 2007; Thompson et al., 2007), a condition with 5-fold increased risk for subsequent development of AD (Petersen et al., 1999; Petersen, 2000). In AD, the hippocampus and entorhinal cortex of the temporal lobes are typically the first structures to degenerate (Braak and Braak, 1991; Thompson et al., 2003). Temporal lobe volume differences are detectable on structural brain MRI through delineation of the hippocampus (Morra et al., 2009) or by tensor-based morphometry (Hua et al., 2008), which plots the 3D profile of volume loss or gain relative to a template. Lower temporal lobe volume is a well known biological marker and risk factor for AD and MCI (Hua et al., 2008), and reflects both cellular atrophy (shrinkage) and overt neuronal loss (Brun and Englund, 1981). In young healthy adults, twin studies attribute ~50% of the temporal lobe volume variation (Brun et al., 2008) and 40–69% of hippocampal volume variation (Peper et al., 2007) to genetic influences.

Late-onset AD is genetically complex; most likely, many genes with small effects contribute to the overall disease phenotype (Tanzi, 1999; Waring and Rosenberg, 2008). Several genetic variants are known to increase the risk for late-onset AD including those in the *CLU* and *PICALM* genes (Harold et al., 2009; Lambert et al., 2009) and most notably the ε4 allele of the *APOE* gene (Farrer et al., 1997); however, the ε4 allele is found in only around 38% of those with AD (relative to 14% of healthy subjects), and these genetic variants do not account for the full genetic risk for late-onset AD (Farrer et al., 1997; Bertram et al., 2007). Risk alleles for AD have been verified by comparing allele frequencies of common polymorphisms between AD patients and healthy controls (Bertram et al., 2007). Here, instead of first comparing the incidence of genetic polymorphisms between diagnostic categories, we ask a distinct but related question: which common genetic polymorphisms influence brain structure in pathological aging? Progressive temporal lobe and hippocampal atrophy may mediate the link between genes and behavioral deficits, so any genes associated with structural degeneration may be a more powerful way to identify mechanisms of disease onset and cognitive decline. In addition, the gene products identified may become future therapeutic targets.

Prior genome-wide analysis using quantitative traits relevant to disease or brain function has been successful, and will likely help in better understanding the etiology of these processes. Genetic variants in the *KIBRA* gene were identified using association to memory performance (Papassotiropoulos et al., 2006) and other genetic variants worthy of further study were implicated through studying activation during fMRI tasks of working memory (Potkin et al., 2009a).

In a large-scale genetic analysis of 742 subjects, we set out to identify common genetic polymorphisms that influence brain structure in the elderly. By enforcing a genome-wide statistical threshold to avoid false positives, and incorporating prior knowledge of genetic mechanisms in biochemical pathways relevant to aging and AD, we identified 2 regions on the genome that are strongly associated with temporal lobe structure. The structure-modifying genetic variants were further assessed by comparing allele frequencies between AD patients and healthy controls, a common method to validate a candidate risk gene (Bertram et al., 2007). The function of the most strongly associated gene, already known from prior studies of glutamate receptors, is highly relevant to learning and memory, and relates to current therapeutic strategies for AD (i.e., memantine drug treatment) (Parsons et al., 2007).

Materials and methods

Sample

Neuroimaging and genetic data were acquired from 818 subjects as part of the Alzheimer's Disease Neuroimaging Initiative (ADNI), a large five-year study launched in 2004 by the National Institute on Aging (NIA), the National Institute of Biomedical Imaging and Bioengineering (NIBIB), the Food and Drug Administration (FDA), private pharmaceutical companies, and non-profit organizations, as a $60 million, public–private partnership. The goal of the ADNI study is to determine biological markers of Alzheimer's disease through neuroimaging, genetics, neuropsychological tests and other measures in order to develop new treatments and monitor their effectiveness, and lessen the time of clinical trials. Subjects were recruited from 58 sites in the United States. The study was conducted according to the Good Clinical Practice guidelines, the Declaration of Helsinki, and U.S. 21 CFR Part 50 — Protection of Human Subjects, and Part 56 — Institutional Review Boards. Written informed consent was obtained from all participants before protocol-specific procedures were performed. All data acquired as part of this study are publicly available (http://www.loni.ucla.edu/ADNI/).

All subjects underwent thorough clinical and cognitive assessment at the time of scan acquisition to determine diagnosis. The mini-mental state exam (MMSE) was administered to provide a global measure of mental status (Cockrell and Folstein, 1988). The clinical dementia rating (CDR) was used to assess dementia severity (Morris, 1993). Healthy volunteer status was determined through MMSE scores between 24 and 30 (inclusive), a CDR of 0, non-depressed, non-MCI, and non-demented. MCI diagnosis was determined by MMSE scores between 24 and 30 (inclusive), a memory complaint, objective memory loss measured by education adjusted scores on the Wechsler Memory Scale Logical Memory II, a CDR of 0.5, absence of significant levels of impairment in other cognitive domains, essentially preserved activities of daily living, and an absence of dementia. Diagnosis of AD was made according to NINCDS-ADRDA criteria for probable AD (McKhann et al., 1984), MMSE scores between 20 and 26 (inclusive), and CDR of 0.5 or 1.0. Definitive autopsy-based diagnosis of AD was not possible.

DNA isolation and SNP genotyping methods

DNA was isolated from B lymphocyte cells taken from blood (Neitzel, 1986) and extracted (Lahiri et al., 1992) using standard procedures. Genomic DNA samples were analyzed on the Human610-Quad BeadChip (Illumina, Inc. San Diego, CA) according to the manufacturer's protocols (Infinium HD Assay; Super Protocol Guide; Rev. A May 2008). Before the initiation of the assay, 50 ng of genomic DNA from each sample was examined qualitatively on a 1% Tris-acetate-EDTA agarose gel for visual signs of degradation. Any degraded DNA samples were excluded from further analysis. Samples were quantitated in triplicate with PicoGreen® reagent (Invitrogen, Carlsbad, CA) and diluted to 50 ng/μl in Tris-EDTA buffer (10 mM Tris, 1 mM EDTA, pH 8.0). 200 ng of DNA was then denatured, neutralized, and amplified for 22 h at 37 °C (this is termed the MSA1 plate). The MSA1 plate was then fragmented with FMS reagent (Illumina) at 37 °C for 1 h and then precipitated with 2-propanol and incubated at 4 °C for 30 min. The resulting blue precipitate was then resuspended in RA1 reagent (Illumina) at 48 °C for 1 h. The samples were then denatured (95 °C for 20 min) and immediately hybridized onto BeadChips at 48 °C for 20 h. BeadChips were then washed and subjected to single base extension and staining. Finally, the BeadChips were coated with XC4 reagent (Illumina), dessicated, and imaged on the BeadArray Reader (Illumina).

Genetic analysis

Genome-wide genotype information was collected at 620,901 markers. Multiple types of genetic variants were genotyped, but only

Please cite this article as: Stein, J.L., et al., Genome-wide analysis reveals novel genes influencing temporal lobe structure with relevance to neurodegeneration in Alzheimer's disease, NeuroImage (2010), doi:10.1016/j.neuroimage.2010.02.068

Single Nucleotide Polymorphisms (SNPs) were included in this analysis. Alleles on the forward strand are reported. Individual markers were excluded from the analysis that did not satisfy the following quality criteria based on previous genome-wide association studies (Wellcome Trust Case Control Consortium, 2007): genotype call rate <95% (42,680 SNPs removed), significant deviation from Hardy–Weinberg equilibrium $P<5.7\times10^{-7}$ (873 markers removed), minor allele frequency <0.01 (60,867 SNPs removed), and a platform-specific recommended quality control score of <0.15 (variable number of SNPs removed across subjects). 546,314 SNPs remained for analysis after quality control. Association was conducted using the Plink software package (Purcell et al., 2007) (version 1.05; http://pngu.mgh.harvard.edu/purcell/plink/) to conduct a regression at each SNP with the number of minor alleles, age, and sex as the independent variables and the quantitative phenotype (temporal lobe or hippocampal volume) as the dependent variable, assuming an additive genetic model.

In addition to a standard regression analysis, a permutation test was conducted to give *P*-values corrected for multiple comparisons across all the SNPs assessed for potential association. First, the effects of age and sex were regressed on the phenotype. The residuals of this regression formed age and sex adjusted phenotypes. Phenotypes (i.e. image data) were randomly swapped between subjects without restriction, and the linear regression analysis without covariates was performed again for each marker and the *t*-statistic of association was saved. This process was repeated 10,000 times to obtain a non-parametric null distribution *for the best SNP*. We note that this is quite a conservative approach, as the SNP's *P*-value is not merely compared to its own association *P*-value in null data (which would be appropriate if it was the only SNP examined). Instead, it is compared with the best (most strongly associated) SNP's *P*-value at each randomization. To assign a corrected *P*-value to a SNP, the *t*-value for association when the data were correctly assigned is compared to the maximum of all the permuted statistics at each iteration.

Genes and ESTs in close proximity to significant SNPs were localized through the UCSC genome browser (Kent et al., 2002) (http://genome.ucsc.edu/) and are shown in Table 1. Results were visualized and linkage disequilibrium (LD) patterns with putative causative mutations in the general population were explored using Haploview (Barrett et al., 2005) (version 4.1; http://www.broad.mit.edu/mpg/haploview/) using allele frequency information from a European population (CEU) derived from the HapMap project (Frazer et al., 2007) (Release 22; http://www.hapmap.org/). Additionally, gene functions and known associations with disease were reviewed using the Online Mendelian Inheritance in Man database (OMIM; http://www.ncbi.nlm.nih.gov/sites/entrez?db=omim) and gene ontology information from the Entrez Gene (http://www.ncbi.nlm.nih.gov/sites/entrez?db=gene) database.

Within-group permutation to control for effects of diagnostic status

To ensure that diagnosis did not confound the analyses, empirical *P*-values were generated using the "–within" flag in Plink. This permutation algorithm randomly swaps phenotypes between individuals, but only within specified subgroups — in this case diagnosis group (AD, MCI, controls). Any effect of group is then built into the null (reference) distribution formed by permutation tests. The linear regression analysis without covariates was performed again for each marker and the *t*-statistic for each marker was saved. This process was adaptively repeated to ensure stable *P*-values (up to 100 million replicates). SNPs that proved unlikely to become significant after a small number of permutations were no longer swapped for computational efficiency as high precision for non-associated (high) *P*-values is not desirable here. The number of times a test statistic met or exceeded the observed test statistic was divided by the total number of permutations performed for that SNP. The effect of diagnosis is therefore preserved in each permuted dataset. In this way, we were able to control for diagnosis in the analyses without the loss of power and multiple testing issues related to analyzing each group separately.

Association controlling for population structure

To control for population substructure, an additional analysis was performed which controls for genetic relatedness. First, a kinship matrix was estimated from the identity-by-state relationship of each subject to each other. A linear mixed effects model was then used to estimate the significance of each SNP to the phenotype of interest controlling for any population structure and also controlling for age and sex according to the formula

$$\boldsymbol{y} = \mathbf{X}\beta + \mathbf{Zu} + \mathbf{e} \quad (1)$$

where *y* is a vector representing the phenotype; X is a matrix of fixed effects containing the additive genetic effect of a SNP, age, sex, and a constant term; β is a vector representing the fixed effect regression coefficients; **Z** is an identity matrix; u is the random effect with $\mathrm{Var}(u) = \sigma^2_g K$, where K is the kinship matrix; and e is a matrix of residual effects with $\mathrm{Var}(e) = \sigma^2_e I$. This analysis was implemented using the Efficient Mixed-Model Association (EMMA; http://mouse.cs.ucla.edu/emma/) (Kang et al., 2008).

Table 1
All SNPs surviving the $P<1\times10^{-5}$ threshold for genome-wide association with temporal lobe atrophy and hippocampal volumes. The two SNPs that survive genome-wide evidence threshold are underlined and *italicized*. Genes are **bolded** when a SNP falls directly within them. MAF is the minor allele frequency. β values give the additive genetic effect from the major allele, after controlling for age and sex. *P*-values in parentheses give the association of SNPs when controlling for diagnostic group using permutations within group. *GRIN2B*: glutamate receptor, ionotropic, *N*-methyl-D-aspartate 2B; *KIAA0743*: neurexin 3; *ZNF326*: zinc finger protein 326; *UTP20*: UTP20, small subunit (SSU) processome component, homolog (yeast).

Chromosome	Gene within ±50 kb	SNP	*P*-value	MAF	Minor allele	Major allele	Position	β
Temporal lobe atrophy								
3p22.1		rs9832461	3.723×10^{-6} (1.441×10^{-5})	0.2369	G	A	39724597	3765.6
3p22.1		rs1527566	2.323×10^{-6} (3.261×10^{-6})	0.2530	C	T	39747455	3757.8
3p22.1		rs9878556	2.899×10^{-6} (7.988×10^{-6})	0.2365	T	G	39771730	3794.3
4p15.1		rs1448284	1.963×10^{-6} (1.318×10^{-6})	0.0302	C	T	32756050	9939.9
12p13.1	***GRIN2B***	rs11055612	2.809×10^{-6} (1.590×10^{-5})	0.4980	T	C	13814595	−3371.6
12p13.1	*GRIN2B*	*rs10845840*	*1.260×10^{-7} (4.033×10^{-7})*	*0.4416*	*T*	*C*	*13822124*	*−3802.2*
14q24.3	**KIAA0743**	rs7155434	7.818×10^{-6} (7.945×10^{-6})	0.2749	C	A	77845059	3643.0
15q22.2		*rs2456930*	*3.142×10^{-7} (1.500×10^{-7})*	*0.3790*	A	*G*	*60474631*	*3843.9*
Hippocampal volume								
1p22.2	*ZNF326*	rs2813746	1.719×10^{-6} (1.054×10^{-5})	0.4550	A	C	90312352	148.1
10p12.33		rs16917919	7.666×10^{-6} (8.684×10^{-5})	0.3737	G	A	19200035	147.6
12q23.2	***UTP20***	rs2290720	2.839×10^{-6} (1.463×10^{-5})	0.4303	A	G	100211174	−148.1
16q21		rs8056650	1.471×10^{-6} (3.167×10^{-5})	0.0698	A	G	58448199	−302.5

Please cite this article as: Stein, J.L., et al., Genome-wide analysis reveals novel genes influencing temporal lobe structure with relevance to neurodegeneration in Alzheimer's disease, NeuroImage (2010), doi:10.1016/j.neuroimage.2010.02.068

MRI analysis methods

Three-dimensional T_1-weighted baseline brain MRI scans were analyzed using tensor-based morphometry (TBM) and an automated hippocampal recognition algorithm as detailed in previous studies (Hua et al., 2008; Morra et al., 2008). Briefly, high-resolution structural brain MRI scans were acquired at 58 ADNI sites with 1.5 T MRI scanners using a sagittal 3D MP-RAGE sequence developed for consistency across sites (Jack et al., 2008) (TR = 2400 ms, TE = 1000 ms, flip angle = 8°, field of view = 24 cm, final reconstructed voxel resolution = $0.9375 \times 0.9375 \times 1.2$ mm^3). Images were calibrated with phantom-based geometric corrections to ensure consistency across scanners. Additional image corrections included (Jack et al., 2008): (1) correction of geometric distortions due to gradient nonlinearity, (2) adjustment for image intensity inhomogeneity due to B1 field non-uniformity using calibration scans, (3) reducing residual intensity homogeneity, and (4) geometric scaling according to a phantom scan acquired for each subject to adjust for scanner- and session-specific calibration errors. Images were linearly registered with 9 parameters to the International Consortium for Brain Imaging template (ICBM-53) (Mazziotta et al., 2001) to adjust for differences in brain position and scaling.

For TBM analysis, the protocol was identical to that of a prior study analyzing the clinical correlates of temporal lobe volume differences (Hua et al., 2008) in a smaller population; since then, genome-wide genotype data was collected. First, a minimal deformation template (MDT) was created for the healthy elderly group to serve as an unbiased average template image to which all other images were warped using a non-linear inverse-consistent elastic intensity-based registration algorithm (Leow et al., 2005; Hua et al., 2008). Volumetric tissue differences were assessed in all individuals by averaging the determinant of the Jacobian matrix of deformation in a bilateral temporal lobe region of interest, manually delineated on the MDT (Fig. 2a). The average of the determinant of the Jacobian matrix multiplied by the volume of the temporal lobe delineated on the template gives the volume of the temporal lobe in each subject. This volumetric difference relative to a population-based brain template served as the temporal lobe volume measure.

For the hippocampal volume analysis, the protocol is identical to that of a prior study assessing hippocampal volume (Morra et al., 2008). Two independent raters reliably delineated the hippocampus in 21 subjects (7 AD, 7 MCI, and 7 healthy elderly). The auto context model, a machine learning algorithm based on AdaBoost (Freund and Schapire, 1997), was used to create a model based on the most predictive features from the images in one of the rater's training sets (Morra et al., 2008). The model was then applied to all other scans in the sample, generating a 3D outline of the hippocampus in the full set of images (Fig. 2b). The average bilateral hippocampal volume served as the hippocampal volume phenotype. To reduce effects of any segmentation errors on the hippocampal volume estimates, we eliminated some subjects with volumes in the extreme lowest and highest percentiles of the full sample (40 lying more than 2 standard deviations below the mean and 1 subjects lying more than 2 standard deviations above the mean).

As expected, the two phenotypes of temporal lobe volume and hippocampal volume were moderately correlated ($r^2 = 0.079$, $P = 1.02 \times 10^{-13}$). The quantitative phenotypes are partially dependent, as both hippocampal and temporal lobe volume reduction occur with normal aging and Alzheimer's disease, but the variance in one explained by the other is low.

Results

Population stratification

Population stratification is a known problem in genetic association analyses, which can produce false-positive or false-negative results (McCarthy et al., 2008). When multiple subpopulations are present in the data (population stratification), spurious associations (or lack of associations) can result from allele frequency differences between populations rather than associations with the phenotype (Lander and Schork, 1994). Self-declared Caucasian (non-Hispanic) subjects represented the vast majority of the genetic data in the Alzheimer's Disease Neuroimaging Initiative sample (91%), so only these subjects ($N = 745$) were included to reduce population stratification effects. It is possible that self-declared ethnicity does not match with true ethnicity, and that substructure exists even within the Caucasian group. To examine this, multi-dimensional scaling (MDS) was used to project the identity-by-state (IBS) relationship of each subject in relation to other subjects to a 2-dimensional space. Substructures in the data, showing genetically more or less related groups, can then be easily visualized (Fig. 1). The MDS results showed that all self-identified Caucasians fell within the same genotypic cluster, confirming the self-report and providing evidence for using only Caucasian subjects to reduce the effects of population stratification (Fig. 1, left). Additionally, the MDS plot identified 2 pairs of subjects as siblings within the Caucasian group (Fig. 1, middle) and otherwise showed some substructure within the data (Fig. 1, right).

Temporal lobe volume in diagnostic groups

Two partially independent phenotypes were analyzed: temporal lobe volume and hippocampal volume, each with a slightly different population sample. Temporal lobe volume was assessed in 173 AD patients (78 female/95 male; mean age ± standard deviation = 75.54 ± 7.66), 361 MCI subjects (130 female/231 male; 75.16 ± 7.29), and 208 healthy elderly subjects (95 female/113 male; 76.07 ± 4.95). Age was not significantly different between groups ($F_{2,739} = 1.172$; $P = 0.3103$), but gender was ($\chi^2(2) = 6.787$, $P = 0.0334$). Hippocampal volume was assessed in 162 AD patients (73 female/89 male; 75.17 ± 7.57), 343 MCI subjects (128 female/215 male; 74.94 ± 7.26), and 193 healthy elderly (91 female/102 male; 76.11 ± 4.97). Age was not significantly different between groups ($F_{2,695} = 1.892$; $P = 0.1516$), but there was a trend in gender differences between the groups ($\chi^2(2) = 5.810$, $P = 0.0547$).

The profile of temporal lobe volume differences was assessed with tensor-based morphometry (TBM; Fig. 2a) which plots, in 3D, the pattern of differences in regional brain volumes, for each brain, relative to a minimal deformation template (MDT) of healthy elderly subjects from this study (Hua et al., 2008). The volume difference for all voxels in a bilateral temporal lobe region of interest was averaged and used as a quantitative phenotype for genomic association, as a summary measure of temporal lobe volume. Hippocampal volume was assessed with an automated recognition program (Fig. 2b) that was trained on 21 manual delineations of the hippocampus by a reliable rater (Morra et al., 2008). The average bilateral hippocampal volume was also used as a quantitative phenotype for genomic association.

As expected, an initial comparison of temporal lobe volume between diagnostic groups showed significant differences between both AD vs. healthy elderly (mean temporal lobe volume in mm^3 ± s.d. 255,483 ± 13,927 vs. 264,405 ± 11,827; $t_{379} = -6.76$; $P = 5.19 \times 10^{-11}$) and MCI vs. healthy elderly (259,501 ± 13,886 vs. 264,405 ± 11,827; $t_{567} = -4.27$; $P = 2.22 \times 10^{-5}$). A comparison of hippocampal volume between diagnostic groups also showed significant differences, as expected, between both AD vs. healthy elderly (mean hippocampal volume in mm^3 ± s.d. 2,713.2 ± 555.4 vs. 3,417.6 ± 531.0; $t_{353} = -12.19$; $P = 2.2 \times 10^{-16}$) and MCI vs. healthy elderly (3,001.6 ± 574.2 vs. 3,417.6 ± 531.0; $t_{534} = -8.27$; $P = 1.1 \times 10^{-15}$).

Genome-wide association

Genome-wide association analysis at 546,314 SNPs using temporal lobe and hippocampal volume as quantitative phenotypes, after controlling for age and sex, revealed two SNPs that survived the genome-wide evidence threshold (Wellcome Trust Case Control

Please cite this article as: Stein, J.L., et al., Genome-wide analysis reveals novel genes influencing temporal lobe structure with relevance to neurodegeneration in Alzheimer's disease, NeuroImage (2010), doi:10.1016/j.neuroimage.2010.02.068

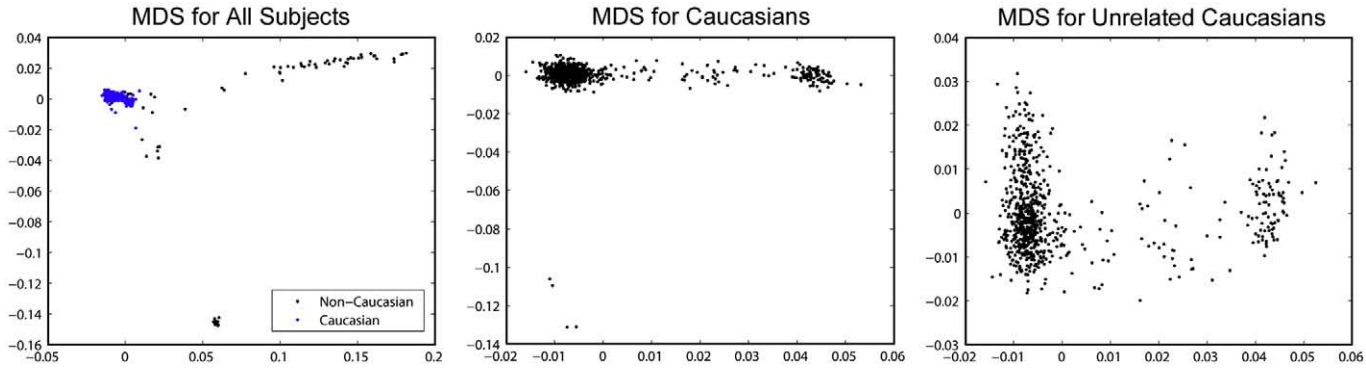

Fig. 1. Multi-dimensional scaling shown in three groups of subjects. Each dot represents a subject, and the distance between dots represents overall genetic similarity. Dots close together represent genetically more similar subjects. Left: MDS for all subjects genotyped as part of the ADNI dataset. Self-declared Caucasians (blue) group together very closely, whereas non-Caucasians (black) do not. Middle: MDS for Caucasian subjects only. Four outliers are seen which represent two sibling pairs. Right: MDS for Caucasian subjects only randomly excluding one person from each of the two sibling pairs. Some substructure is evident. (For interpretation of the references to color in this figure legend, the reader is referred to the web version of this article.)

Consortium, 2007; Sabatti et al., 2009) of $P<5\times10^{-7}$ (Fig. 3a). Information on SNPs surviving a more liberal threshold of $P<1\times10^{-5}$ and their closest genes (within ±50 kb) is presented in Table 1.

To assess the corrected significance level of these findings, we constructed a quantile–quantile plot of sorted *P*-values based on a $\log_{10}$ scale (McCarthy et al., 2008) (Fig. 3b). No inflation of observed vs. expected *P*-values (black line) was found, as shown through these plots and by calculation of variance inflation factors (Bacanu et al., 2000), λ, which do not differ greatly from 1 (temporal lobe volume $\lambda=1.021$, hippocampal volume $\lambda=1.013$). This demonstrates that the data generally follow the null hypothesis of no association and only deviate in the far tails of the distribution. Population stratification is therefore again unlikely to account for the results.

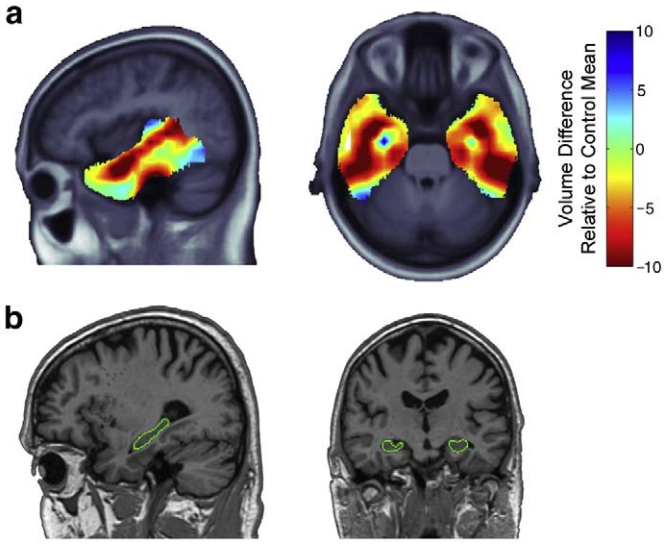

Fig. 2. Temporal lobe and hippocampal volume measures. (a) An unthresholded color-coded map shows the average percent volume reduction of AD patients ($N=173$) relative to a standard mean brain image based on identically scanned healthy subjects, in a temporal lobe region of interest overlaid on the population-based template. Here the temporal lobe is ~10% smaller in red regions than the average volume in matched controls. The average bilateral temporal lobe volume was used as a quantitative phenotype for the genomic association analysis, prior to fine-scale voxel-based genetic association mapping. (b) Automatic delineation of the hippocampus in a representative healthy elderly subject (the hippocampal boundary is shown in green). The average of the left and right hemisphere hippocampal volumes was used as a quantitative phenotype for the genomic association analysis. (For interpretation of the references to color in this figure legend, the reader is referred to the web version of this article.)

Both SNPs that survived the genome-wide evidence threshold were found using the temporal lobe volume phenotype. One SNP, rs10845840 ($P=1.260\times10^{-7}$), is located on chromosome 12 within an intron of the *GRIN2B* gene, which encodes for the regulatory subunit 2B (NR2B) of the NMDA glutamate receptor. An additional SNP, rs11055612, strongly associated with the temporal lobe volume phenotype ($P=2.809\times10^{-6}$) is also located in an intron of the *GRIN2B* gene and in high LD with rs10845840 ($r^2=0.872$). The other SNP which survived the genome-wide evidence threshold, rs2456930 ($P=3.142\times10^{-7}$), lies in an intergenic region of chromosome 15. Upon randomly removing two subjects, one from each of the sibling pairs identified above, the results were changed very little and still survived the genome-wide evidence threshold ($P=1.715\times10^{-7}$ for rs10845840; $P=2.191\times10^{-7}$ for rs2456930; $N=740$). Additionally, because some population substructure was identified (Fig. 1, right) an analysis was conducted using a mixed-model approach that controls for genetic relatedness (Kang et al., 2008). The two SNPs identified here remained significant in this analysis ($P=1.463\times10^{-7}$ for rs10845840; $P=3.762\times10^{-7}$ for rs2456930; $N=742$) clearly showing that population substructure is not accounting for the results. These findings also survive the genome-wide evidence threshold after controlling for diagnostic group by permuting phenotype values within each of the three diagnostic categories ($P=4.033\times10^{-7}$ for rs10845840 and $P=1.500\times10^{-7}$ for rs2456930; $N=742$). After correction for multiple comparisons using permutation testing, both SNPs have trend-level association (corrected $P=0.05419$ for rs10845840 and corrected $P=0.1369$ for rs2456930; $N=742$).

Other genes of interest (Table 1) were identified with both the temporal lobe volume and hippocampal volume phenotypes at a more liberal threshold of $P<1\times10^{-5}$. These genes include *RNF220*, *UTP20*, and *KIAA0743*. *RNF220* and *UTP20* are largely unstudied, but they fall into functional groups of metal binding (*RNF220*) and suppression of cell proliferation (Schwirzke et al., 1998) (*UTP20*). *KIAA0743* is also known as *NRXN3* (neurexin 3) and is involved with axon guidance and cell adhesion (Ushkaryov et al., 1992). Additionally, SNP rs1448284 is located on chromosome 4 within an expressed sequence tag (EST; GenBank accession DA204899) showing expression in the brain (Kimura et al., 2006); however, it is not in LD with any RefSeq (a curated Reference Sequence database) gene. Additional interesting SNPs were identified in intergenic regions which were not close to genes or ESTs.

To determine how the different genotypes of the most associated SNPs affected brain volumes, boxplots were created for each of these SNPs (Fig. 4). As expected, an additive genetic effect is clearly evident

Please cite this article as: Stein, J.L., et al., Genome-wide analysis reveals novel genes influencing temporal lobe structure with relevance to neurodegeneration in Alzheimer's disease, NeuroImage (2010), doi:10.1016/j.neuroimage.2010.02.068

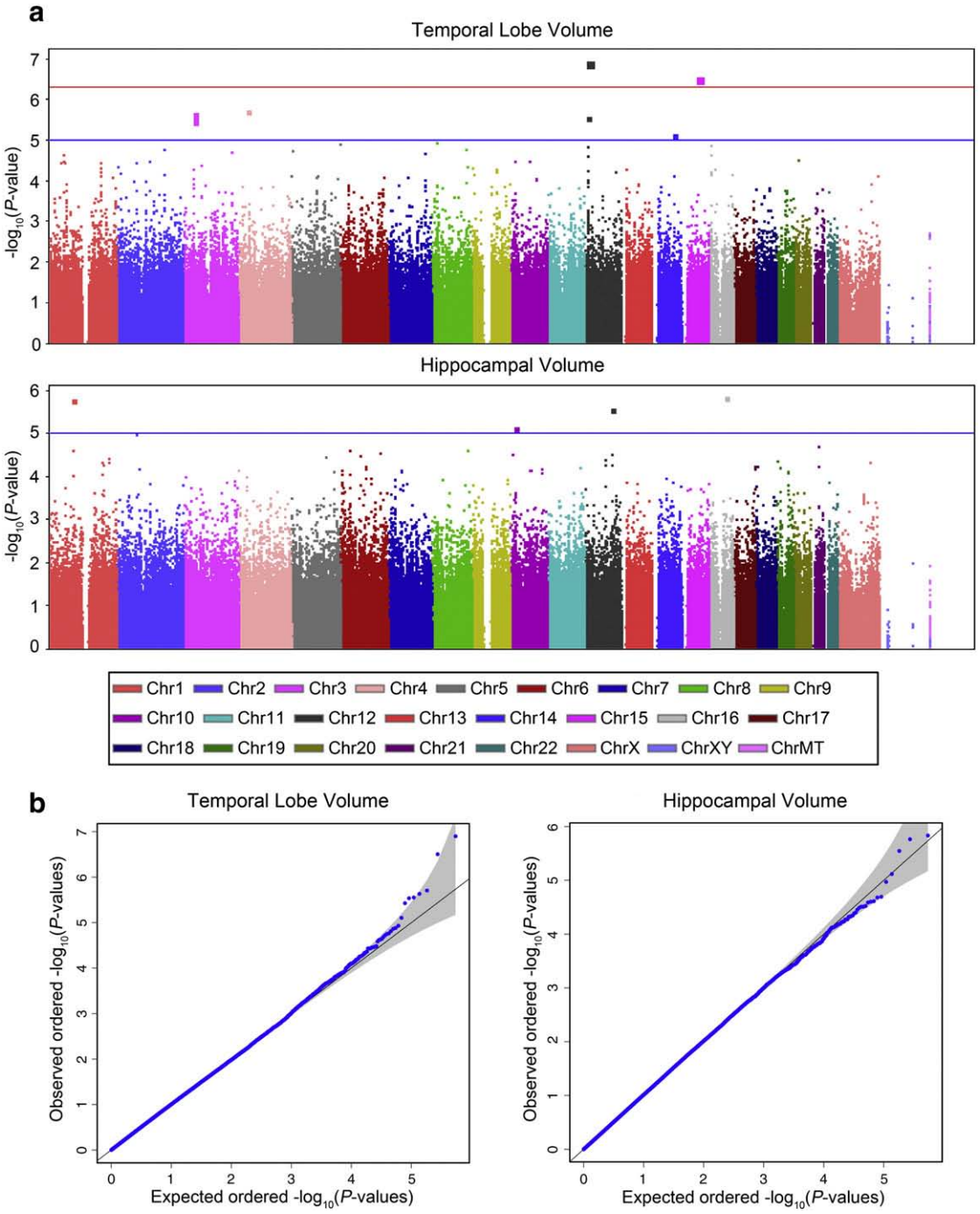

Fig. 3. Association of 546,314 SNPs to temporal lobe and hippocampal volume in $N = 742$ and $N = 698$ subjects, respectively. (a) The *x*-axis moves along each base pair of each chromosome (identified in color in the key) and the *y*-axis gives the $-\log_{10}$ of the *P*-value for association. The red line corresponds to the genome-wide evidence value of $P = 5 \times 10^{-7}$; all points above this line represent SNPs that are strongly associated with the phenotype. The two SNPs which survive the genome-wide evidence threshold are rs10845840 on chromosome 12 and rs2456930 on chromosome 15. The blue line corresponds to a more liberal threshold identifying genes of interest ($P = 1 \times 10^{-5}$). (b) A quantile–quantile plot shows the distribution of *P*-values in this sample vs. the *P*-values expected under the null hypothesis of no association (blue dots). The black line and grey shading shows 95% confidence intervals of the expected distribution. (For interpretation of the references to color in this figure legend, the reader is referred to the web version of this article.)

with the lowest phenotype value resembling a risk genotype (T allele for rs10845840 and G allele for rs2456930).

Presence of risk alleles in diagnostic groups and association to cognitive testing

After detecting their effect on brain structure, we tested if the allele frequencies for the two most associated SNPs identified in this study were over-represented in impaired vs. healthy subjects (AD and MCI vs. healthy elderly) in all 745 Caucasian (non-Hispanic) subjects with genomic data. Intriguingly, the adverse genotype of the SNP within rs10845840 (in the glutamate receptor *GRIN2B* gene) was significantly over-represented in MCI and AD ($\chi^2 = 4.242$; OR = 1.273; $P = 0.039$). The allele frequency of the other SNP, rs2456930, was not significantly different between diagnostic groups ($\chi^2 = 0.760$; OR = 0.902; $P = 0.383$). Additionally, MMSE scores were

Please cite this article as: Stein, J.L., et al., Genome-wide analysis reveals novel genes influencing temporal lobe structure with relevance to neurodegeneration in Alzheimer's disease, NeuroImage (2010), doi:10.1016/j.neuroimage.2010.02.068

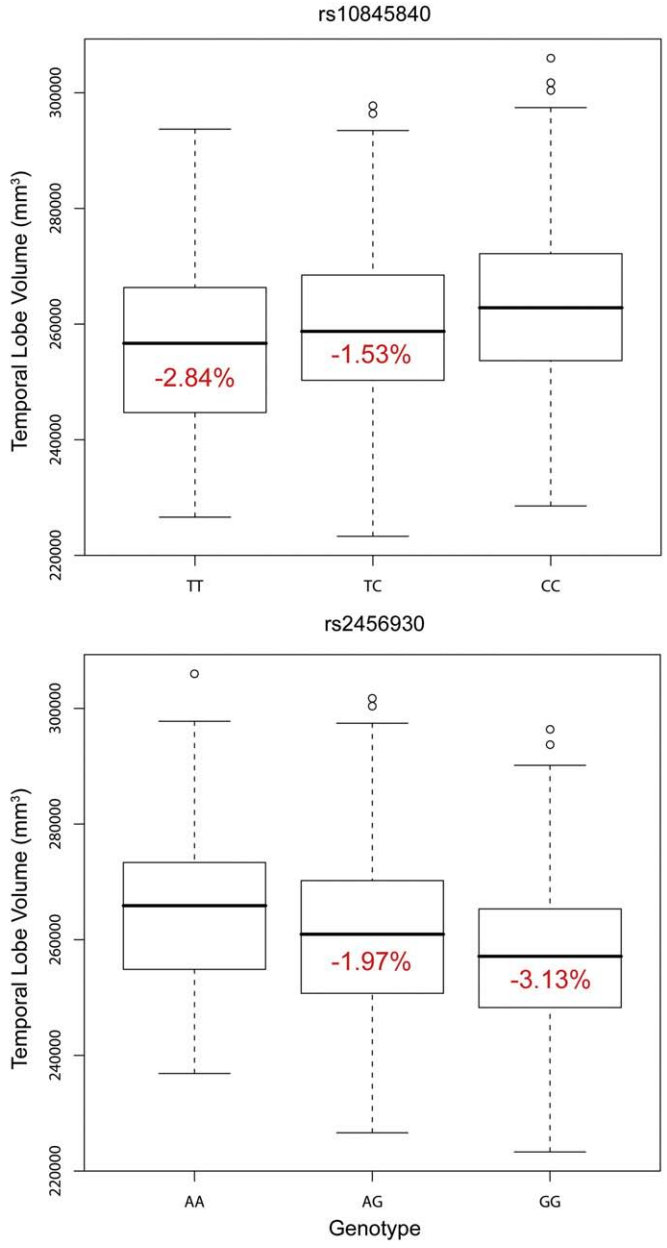

Fig. 4. Box plots of temporal lobe volume grouped by genotype at most associated SNPs. Box plots show the median value (horizontal line), first and third quartiles (box), 1.5 multiplied by the interquartile range (whiskers), and outliers beyond that range (open dots) for each genotype group. Each box plot is in the order homozygous minor allele (TT or AA), heterozygous (TC or AG), homozygous major allele (CC or GG) at each SNP. The frequencies of each genotype are 12.96%, 49.53%, 37.52% for rs2456930, and 18.73%, 50.67%, 30.59% for rs10845840. Red numbers show the difference between the mean phenotype value of the higher-volume genotype group vs. the mean phenotype value of each other genotype group. (For interpretation of the references to color in this figure legend, the reader is referred to the web version of this article.)

associated with the adverse genotype of the *GRIN2B* SNP rs10845840 ($t=-2.114$; $P=0.035$) showing that risk alleles are associated with a negative effect on global cognitive function. However, MMSE scores were not associated with rs2456930 ($t=-0.3373$; $P=0.736$).

Linkage disequilibrium patterns with putative causative genetic variants

The polymorphisms identified here could serve as proxies for association tests to causative SNPs not directly genotyped in this experiment. The HapMap database gives the linkage disequilibrium, or correlation between the presence of two alleles in a population, for many more SNPs across the genome than were genotyped in this experiment. We identified three functional SNPs within the *GRIN2B* gene (including adjacent regulatory regions) that were also genotyped in a European population in the HapMap database. Functional SNPs were defined as SNPs in untranslated regions with potential to affect transcription (3′ or 5′ UTR), SNPs in exons that change the amino acid or prematurely end translation of the protein (coding non-synonymous), and SNPs in splice sites. The SNP in the *GRIN2B* gene identified here (rs10845840) had low correlation to three SNPs in the 5′ UTR of the *GRIN2B* gene: rs1805502 ($r^2=0.0060$), rs1805476 ($r^2=0.096$), rs890 ($r^2=0.1$). Other functional SNPs exist within the *GRIN2B* gene but are not available from the HapMap database version used here (Release 22).

Estimation of sample size needed for replication

To estimate how many subjects would be needed to replicate the finding, conditional on the dataset used, that these genetic variants are associated with temporal lobe structure, we took a resampling approach. Three subjects, one from each diagnostic category (AD, MCI, and healthy control), were randomly picked and removed from the analysis and the *P*-value for each of the most associated SNPs was calculated. The process was repeated until no more subjects remained in the diagnostic category with the least number of subjects (173 AD subjects). To estimate confidence intervals for this estimate, the resampling was repeated 1000 times. 95% confidence intervals were based on the 2.5th and 97.5th percentiles of the resampled distribution (Fig. 5). Fewer than 323 and <223 subjects would be required to replicate the effect of rs10845840 and rs2456930, respectively, with 95% confidence in a new sample at a significance level of $P<0.025$ (a nominal $P<0.05$, Bonferroni corrected for two independent tests). We note that the standard $P<0.05$ level rather than the genome-wide threshold would be applicable to a replication sample, as a prior hypothesis regarding the specific gene exists.

Voxel-based genetic mapping localizes the effect of SNP rs10845840 within the temporal lobes

The phenotype used initially for the genome-wide search was the overall bilateral volume of the temporal lobes. This phenotype proved useful for finding genomic markers highly associated with the temporal lobe; however, it does not provide the spatial localization of the SNP's effect on the temporal lobe volume. To further investigate this, the difference in temporal lobe volume relative to a standard template was assessed at every voxel in the temporal lobe through TBM, a widely-used method for mapping the 3D profile of brain volumetric differences in human populations (Hua et al., 2008). Temporal lobe volume differences at each voxel were regressed on the number of minor alleles at SNP rs10845840, after adjusting for simultaneous effects of age, and sex, at all voxels, across all subjects. The *P*-value of the genetic association to rs10845840 for each voxel was then plotted, and is shown in Fig. 6. To correct for multiple comparisons across voxels, a False Discovery Rate (Benjamini and Hochberg, 1995; Genovese et al., 2002) correction of $q=0.05$ was used to establish a critical *P*-value threshold of 0.0257. With this approach, on average, only 5% of the suprathreshold voxels in a map of this kind will be false positives; in other words, it is expected that the voxel-by-voxel genetic associations are true associations at 95% of the suprathreshold voxels shown. The SNP has wide ranging effects across the temporal lobe, but the strongest effects are on the bilateral temporal poles and in the medial temporal lobes, bilaterally.

It is also of interest to know if the genetic association between the *GRIN2B* glutamate receptor gene variant and brain volumes can be found within each diagnostic group: controls, MCI, and AD patients. We computed 3 separate maps of the genetic association between the *GRIN2B* glutamate receptor gene variant and brain volumes in healthy

Please cite this article as: Stein, J.L., et al., Genome-wide analysis reveals novel genes influencing temporal lobe structure with relevance to neurodegeneration in Alzheimer's disease, NeuroImage (2010), doi:10.1016/j.neuroimage.2010.02.068

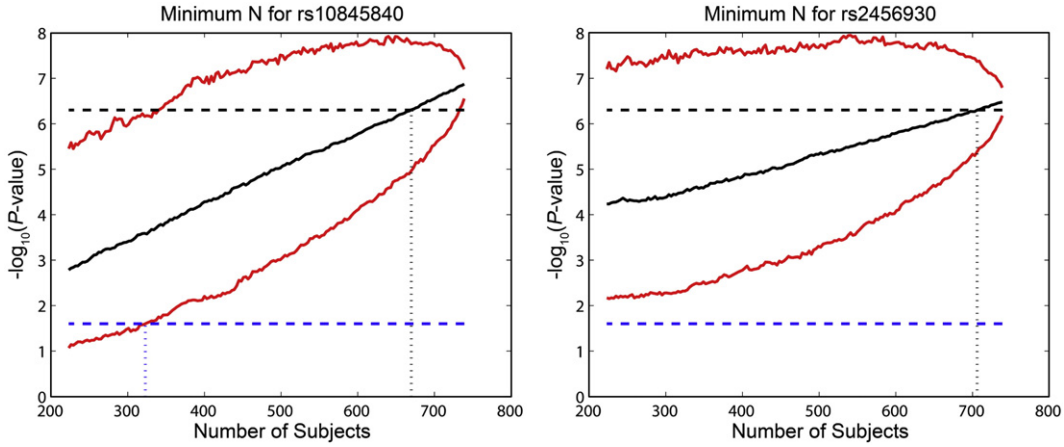

Fig. 5. The minimal number of subjects needed to detect the effect of the most significant SNPs was estimated with a resampling approach. Subjects were randomly removed from each of the diagnostic categories until none was left in a category, and the association *P*-value of the SNP was calculated. This process was repeated 1000 times, to estimate 95% confidence intervals (red lines). The median *P*-value of the repetitions for each number of subjects removed is shown as the solid black line. The dashed black line represents the genome-wide evidence level ($P = 5 \times 10^{-7}$). The dashed blue line represents the replication significance threshold ($P = 0.025$). The dotted blue line shows the estimated minimum sample size that would be required to detect a replication of the finding with 95% confidence ($N = 323$ and <223 for rs10845840 and rs2456930, respectively). The dotted black line shows the median sample size needed for genome-wide support ($N = 670$ and 706 for rs10845840 and rs2456930, respectively). (For interpretation of the references to color in this figure legend, the reader is referred to the web version of this article.)

elderly controls, MCI, and AD patients, separately. For all 3 groups, a cumulative distribution function plot of the observed *P*-values in each of the diagnostic groups is shown in Fig. 7. This figure shows the cumulative distribution of *P*-values in the temporal lobe (see Fig. 6) for all AD, MCI, and healthy elderly subjects separately. In these plots, the curves that rise more sharply than the reference curve ($y = 20x$)

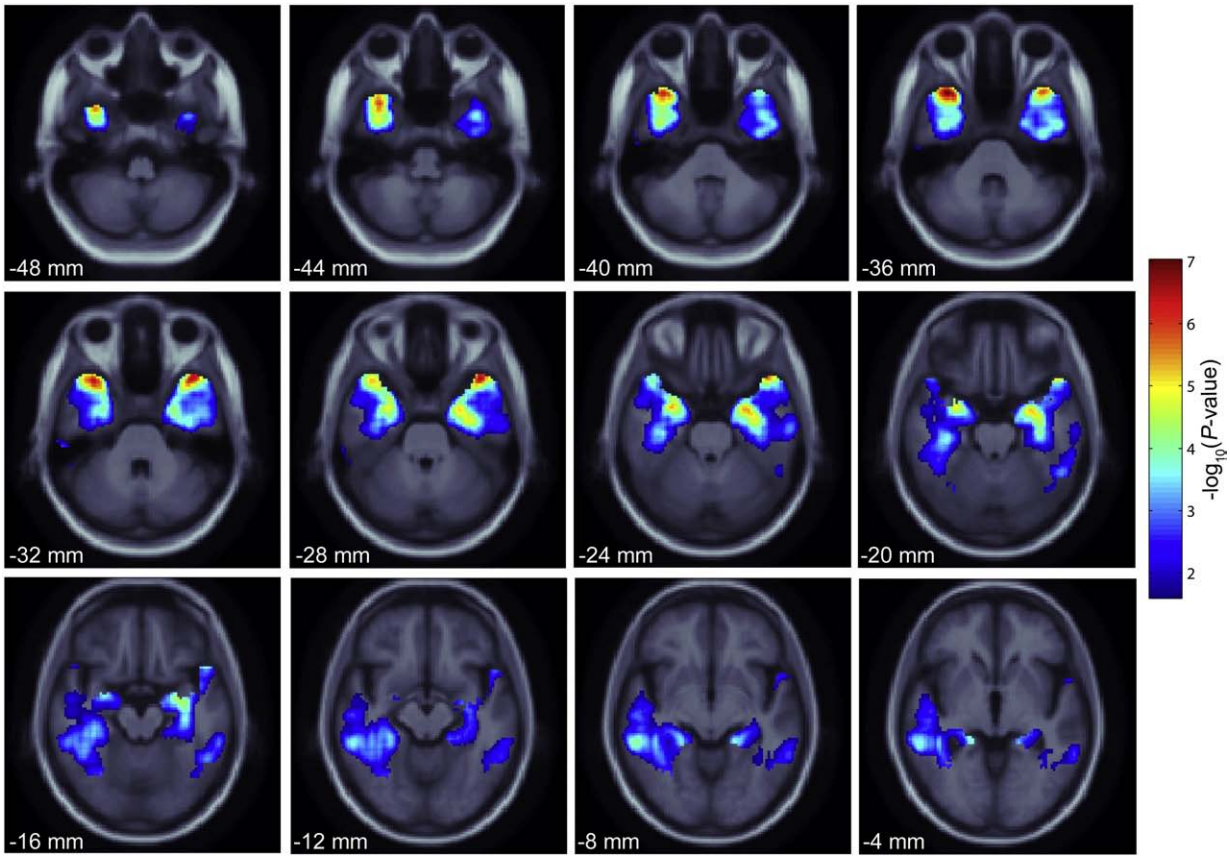

Fig. 6. A voxelwise representation of significant influences of the SNP rs10845840, a genetic polymorphism of the glutamate receptor *GRIN2B* gene, on volumetric differences in the temporal lobe. Indicated in color are brain regions where volumes are statistically associated with variants in the glutamate receptor gene, in 742 subjects, overlaid on a population specific template. Using a convention that is standard in brain mapping, the map was thresholded at an FDR *q*-value of 0.05 across voxels of the temporal lobe, and the overall map is significant after correction for multiple spatial comparisons, and controls the expected number of suprathreshold false positive voxels (i.e., voxels where the association is spurious) at 5% of the total. Z-coordinates in MNI space are shown for each axial slice going from inferior to superior every 4 mm. The frontal lobes are at the top of each panel and the occipital lobes are at the bottom. The images are in radiological convention (left of the image is the right side of the subject). Significance is shown as $-\log_{10}$(*P*-value), with warmer colors representing more significant influence of the SNP on regional temporal lobe volume. (For interpretation of the references to color in this figure legend, the reader is referred to the web version of this article.)

Please cite this article as: Stein, J.L., et al., Genome-wide analysis reveals novel genes influencing temporal lobe structure with relevance to neurodegeneration in Alzheimer's disease, NeuroImage (2010), doi:10.1016/j.neuroimage.2010.02.068

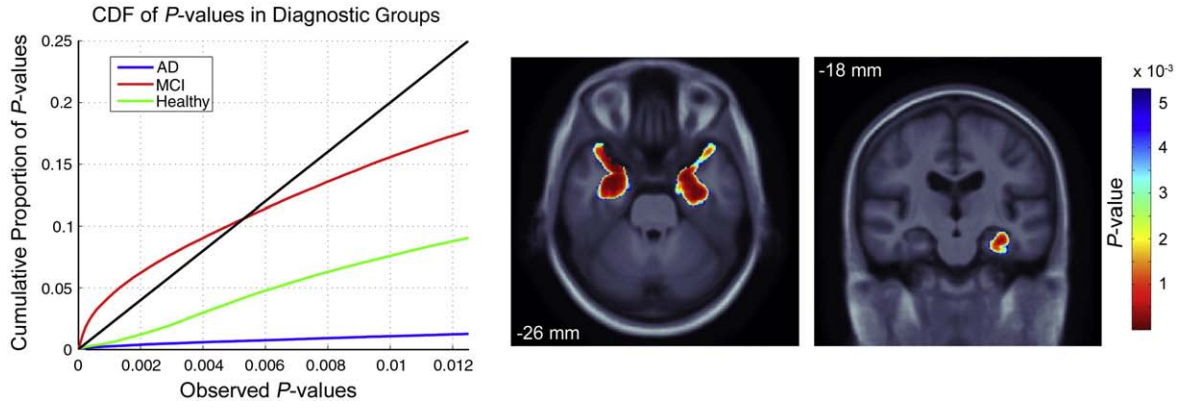

Fig. 7. The cumulative distribution function of *P*-values in the voxelwise genetic association map of SNP rs10845840 (genetic variation in the glutamate receptor) within diagnostic groups and localization of significance in the MCI group. Left: The diagnostic groups here are distinguished according to the color of the line. The black line represents the threshold that curves must cross, to control the false discovery rate at 5%. The maps of genetic association are considered to be significant in the MCI sample because the curve passes above the $y = 20x$ black line. This means that false positives in the maps of genetic association are likely to be occurring at less than 5% of the suprathreshold voxels shown. Middle and right: The voxelwise association overlaid on a subject specific template in both axial (middle; MNI *Z*-coordinate shown) and coronal (right; MNI *X*-coordinate shown) views thresholded to only show significant voxels. (For interpretation of the references to color in this figure legend, the reader is referred to the web version of this article.)

are considered to show significant effects after the conventional correction for multiple spatial comparisons, because they find associations at a rate that is at least 20 times the rate that would be expected by chance if all genomic data were null and showed no association. As shown, only the MCI group passes the FDR threshold of $q = 0.05$ with a critical *P*-value threshold of 0.0053. The MCI group also has the greatest number of subjects.

Interactions with apolipoprotein E (APOE) ε4 allele

The ε4 allele of the *APOE* gene is a well-validated genetic risk factor for AD (Farrer et al., 1997), and we and others have previously found that this allele is associated with temporal lobe atrophy (Hua et al., 2008) and with the rate of hippocampal atrophy (Morra et al., 2009). Excluding all *APOE* ε2 allele carriers, we tested the additive genetic effect of carrying an *APOE* ε4 allele (controlling for age and sex) on temporal lobe structure using a voxelwise approach. As expected, this was significant after correcting for multiple comparisons through FDR (critical $P = 0.000431$; $q = 0.05$; $N = 619$). We then tested whether there was a significant interaction between (1) the additive effect of the risk allele at SNP rs10845840 in the *GRIN2B* gene, and (2) the additive effect of the *APOE* ε4 allele, in terms of their statistical effect on temporal lobe volume differences. A multiple regression model predicting temporal lobe volume differences based on the rs10845840 genotype, *APOE* ε4 genotype, and the interaction of the two (controlling for age and sex) did not survive multiple comparisons correction using FDR at $q = 0.05$, suggesting that epistatic interactions between *APOE* ε4 and *GRIN2B* do not account for our findings.

Discussion

We have identified here two common polymorphisms that are associated with temporal lobe volume with genome-wide support in a large cohort of elderly subjects, assessed with brain imaging and genome-wide scanning. We also identified several potential candidate genes associated with both temporal lobe and hippocampal volume. We identified one SNP within an intergenic region on chromosome 15 which is strongly associated with temporal lobe volume. The most strongly associated polymorphism was within the *GRIN2B* gene, which encodes the NR2B subunit of the NMDA receptor, and is a promising functional candidate considering the prior evidence of its involvement in learning and memory, structural plasticity of the brain, and in characteristic features of AD and neurodegeneration, including as a therapeutic target receptor. NMDA receptors have long been implicated in long-term potentiation, a key process in learning and memory, and over-expression of the *GRIN2B* glutamate receptor gene enhances learning and memory in mice (Tang et al., 1999). Synaptic plasticity mediated through NMDA receptors also causes structural remodeling of neurons, which reinforces these connections (Lamprecht and LeDoux, 2004). Pharmaceutical blockade of NMDA receptor channels can limit cell death induced by excitotoxicity (Kemp and McKernan, 2002; Parsons et al., 2007). In addition, the relative prevalence and location of the NR2B subunit within the synapse is age-dependent. In early postnatal development, there is greater prevalence of the NR2B subunit, and its distribution shifts toward extrasynaptic locations with aging (Yashiro and Philpot, 2008).

In addition, we performed fine-scale voxel-by-voxel mapping of associations between this genetic polymorphism and brain structure. The genes identified here were found based on gross summaries of anatomy, and stringent genome-wide evidence. However, we subsequently used a voxel-based mapping method to assess, at each point in the brain, the statistical association between rs10845840 and variations in brain structure. This clarified the anatomical specificity and localization of the gene effects, revealing strong effects in the bilateral temporal poles and bilateral medial temporal lobes. *In situ* hybridization in post-mortem human brain has revealed high expression of GRIN2B mRNA within pyramidal cells of the temporal cortex and hippocampus (Schito et al., 1997; Allen Institute for Brain Science, 2009), consistent with this SNP having effects in these regions.

These findings may add another piece to the multifactorial genetic puzzle of late-onset AD. Late-onset AD is hypothesized to be influenced by many genes, each with a relatively small effect (Tanzi, 1999; Waring and Rosenberg, 2008). Difficulties in finding these genes may arise from the heterogeneous nature of the disease, which can lead to groups of subjects with the same diagnosis but with different genetic architectures. Here, we use a different approach by studying a phenotype that is biologically based and is strongly associated with the disease. We note that the risk allele identified in the *GRIN2B* gene is over-represented in patients with AD and MCI. It passes the genome-wide support threshold for association with temporal lobe volume deficits, which are a known risk factor for AD. The polymorphisms identified here also have relatively small effect: rs2456930 decreases temporal lobe volume, on average, by 1.473% per risk allele, and rs10845840 decreases temporal lobe volume by 1.457% per risk allele. Each of these genetic variations may contribute somewhat to the as yet unmodeled sources of

Please cite this article as: Stein, J.L., et al., Genome-wide analysis reveals novel genes influencing temporal lobe structure with relevance to neurodegeneration in Alzheimer's disease, NeuroImage (2010), doi:10.1016/j.neuroimage.2010.02.068

heritability of Alzheimer's disease beyond the currently accepted risk alleles, such as *APOE* ε4 (Maher, 2008; McCarthy et al., 2008). A combined approach of studying genetic risk for AD through diagnosis, neuroimaging and structural endophenotypes may result in progress in discovering genetic contributors to late-onset AD.

The image pre-processing conducted here used a 9 parameter linear registration step that matches the position and scales the size of each brain to the MDT. In general, we use 9 parameter registration in our cross-sectional studies of Alzheimer's disease because head size and brain size vary so widely across subjects; the temporal lobe tends to be more vulnerable to atrophy than the rest of the brain, so there is still substantial residual atrophy in AD vs. controls even after adjusting for brain size. Because of this, temporal lobe atrophy is typically easier to detect after controlling for overall brain volume, because the effects of wide variations in head size have been largely removed. In addition, work by Paling et al. (2004) has advocated the use of 9 parameter linear registration, especially in multi-site imaging studies, as it can correct for scanner voxel size variations in large studies involving multiple sites, scanners, and acquisition sequences, such as this one (these are typically mild and may result in variations of 1–3% in brain volume, but they add to measurement error).

Even so, as we have noted in our prior studies (Brun et al., 2009), there is however some evidence for non-proportional scaling of brain subregions relative to the overall size of the brain (Toro et al., 2008). In all stereotaxic studies (e.g., those producing voxelwise maps), this may confound the interpretation of apparently localized brain differences between groups. Put another way, the fraction of the brain that a specific brain substructure is expected to occupy may be larger (or smaller) in a smaller brain. Such an effect can be modeled by including brain volume as a regressor in the scaled Jacobian maps, perhaps after logarithmic transformation of both variables. For a full analysis of this effect, please see Jancke et al. (1997), Thompson et al. (2002) and Brun et al. (2009). This power law effect is relevant to all morphometric studies as regional brain volume is always somewhat affected by the overall size of the brain, and it cannot be ruled out that SNPs influencing subregional volumes do so because they influence the overall size of the brain, if the relative volumes of the brain substructures follow a (nonlinear) power law.

Hippocampal volumes proved to be a less informative phenotype than temporal lobe volume. Hippocampal volumes, though widely studied in a genetic context (Seshadri et al., 2007), are only moderately heritable (Peper et al., 2007) most likely due to the large environmental influence as the hippocampus is a highly plastic structure — responsive to individual experiences. Additionally, though we have used new and reliable delineation methods for automatically delineating the hippocampus in the MRI scans (Morra et al., 2009), it remains one of the most difficult structures to accurately model due to the resolution of the MRI scans and the small intensity differences between the structure and surrounding tissue.

One previous genome-wide association study of brain structure (Seshadri et al., 2007) found that SNPs with associations with temporal brain volume and hippocampal volume, but its power was limited as it examined related individuals, had few hippocampal volumes, and low genomic coverage. Those temporal lobe SNPs identified in the Seshadri study were either not identified or not replicated here. rs5028798 was not directly genotyped in our sample and no good proxy in HapMap was identified; rs2143881 was neither directly genotyped in our sample nor in HapMap; rs2793772 was not directly genotyped in our sample but was genotyped in HapMap with a good proxy rs1104973 ($r^2 = 1$) but was not replicated ($P = 0.6964$); rs10497352 was directly genotyped in our sample but was not replicated ($P = 0.6476$); rs1433527 was directly genotyped in our sample but was not replicated ($P = 0.9804$). Those hippocampal SNPs identified in the Seshadri study were not identified here. rs9293140 and rs1963442 were neither directly genotyped in our sample or in HapMap.

The sample sizes examined here are extremely large for an imaging study (this is one of the largest brain imaging studies to date), but are smaller than other genome-wide association studies that have not used brain scanning (Wellcome Trust Case Control Consortium, 2007). Several factors empower the design. Scans of 742 healthy elderly control, MCI, and AD subjects allowed accurate structural measurements across a broad phenotypic range. The genome-wide analyses were not split within diagnostic groups as the goal was to present as broad a phenotypic continuum (Petersen, 2000) as possible. Though it is possible that diagnostic groups represent distinct genetic backgrounds and may therefore confound the interpretation of our results, here we operate under the hypothesis that associations are evident regardless of diagnostic group, but may be more pronounced in disease (Gottesman and Gould, 2003; Cannon and Keller, 2006). In interpreting findings in this mixed cohort, it cannot be ruled out that the SNP effects are influencing the normal aging process independently of AD pathology. In fact, the SNP effects may even be present in young adults, prior to substantial brain aging. Conversely, it cannot be ruled out that such associations are driven by the presence of different diagnostic categories, and might not be found if only normal subjects were examined. In the future, when the sample sizes are greatly increased as more imaging and genetic data are collected, it should be possible to further stratify the image database to understand (1) which specific subpopulations show a detectable SNP effect, and (2) which processes (AD, aging, early development, or all of them) are influenced by the SNPs of interest. At present we have a more restricted goal of finding SNPs that influence brain structure in a mixed cohort of healthy and ill subjects, including those with AD and those who are healthy. Treating this cohort as a continuum is arguably more defensible than (for example) studying a mixed cohort of subjects with a Mendelian genetic illness (such as Fragile X) and controls. This is because for Alzheimer's disease, a continuum is arguably evident in that some of cellular processes characteristic of AD (e.g., increased cerebral amyloid load) are typically present to some degree in those not yet diagnosed (Braskie et al., in press; Frisoni et al., 2010). For example, healthy elderly subjects often show some hallmarks of AD pathology at a subclinical level (amyloid plaques and tau neurofibrillary tangles) that can be detected on imaging and negatively correlate with cognitive status (Braskie et al., in press; Small et al., 2009). As such, the effect of pathology on the SNP associations cannot be disentangled easily by focusing only on controls, as many harbor pathology at a subclinical level. Additionally, the boundary between MCI and AD is based on cognitive tests and observations of daily living that are easy to assess clinically, not biologically based boundaries (Petersen, 2000). The continuum from healthy aging to mild impairment to disease gives the broadest phenotypic range and therefore the highest power to detect the genetic determinants of brain volume in old age, including variants that may have relevance to AD. Therefore splitting between diagnostic groups is likely to reduce power through both fewer subjects and a smaller phenotypic range (Cannon and Keller, 2006). Even so, using a permutation algorithm we found that the findings exist regardless of diagnostic group. Additionally, the use of continuous traits (instead of discrete diagnostic categories) may also better reflect the underlying biology than clinical diagnosis alone (Potkin et al., 2009b).

In this study we used a genome-wide evidence threshold of $P < 5 \times 10^{-7}$ as in other genome-wide association studies (Wellcome Trust Case Control Consortium, 2007; Sabatti et al., 2009) querying multiple phenotypes. We refer in this paper to genome-wide evidence or support rather than genome-wide significance because there is not yet a universal consensus on how to define an appropriate significance threshold. We used permutation testing in which the imaging data is permuted across subjects and all SNPs are tested to estimate the probability that so high a *P*-value for association could have occurred by chance. This is determined by keeping the same set

Please cite this article as: Stein, J.L., et al., Genome-wide analysis reveals novel genes influencing temporal lobe structure with relevance to neurodegeneration in Alzheimer's disease, NeuroImage (2010), doi:10.1016/j.neuroimage.2010.02.068

of SNPs in each subject, but randomizing the assignment of images to subjects. After conducting associations with all the SNPs, the lowest *P*-value is retained. This procedure can be used to determine a significance threshold that incorporates the fact that SNPs within the same subject are not independent (due to linkage disequilibrium). The two SNPs reported here have a permutation-corrected significance level of $P=0.05419$ for rs10845840 and $P=0.1369$ for rs2456930. The first of these results can be considered to mean that the *GRIN2B* variant associates with the phenotype so strongly that only 1 in 20 times would any SNP at all be so strongly associated in completely null data. This is therefore evidence supporting that the association did not occur by chance.

More recent work has proposed an additional argument, suggesting that a genome-wide significance threshold should account for not just the markers directly measured as part of the experiment, but rather the variation of the entire genome (Dudbridge and Gusnanto, 2008). Such an approach is more conservative; it is based on the premise that the subset of SNPs chosen for genotyping (which depends on the chip and the density of genotyping) could have been a "lucky" choice that came up with a high significance hit, and as such one should control for all genomic variants, even if they were not in fact genotyped in the current experiment. Such a line of argument suggests a genome-wide significance threshold of $P<7.2\times10^{-8}$.

Regardless of the genome-wide significance criterion, the gold standard for determining if hits are true positives is replication. Additional replication of this study's findings is necessary. Work is actively ongoing through the Enhancing NeuroImaging Genetics through Meta-Analysis (ENIGMA) Network (Thompson and Martin, 2010) to find collaborations to replicate the findings presented here. Using a re-sampling approach, we estimate that fewer than 323 and <223 subjects will be needed to replicate the effect of rs10845840 and rs2456930, respectively, in a new sample at a reduced prior hypothesis significance level with 95% confidence. In addition to statistical validation, functional validation is also necessary to understand the mechanism by which these polymorphisms contribute to temporal lobe volume differences (McCarthy et al., 2008). First, it is necessary to determine what the causative polymorphism is within the gene. rs2456930 resides in an intergenic region on the genome, so further characterization of the functional significance of this region is needed. rs10845840 lies in an intron of the *GRIN2B* gene and is not in LD with more finely mapped potential causative mutations from a European sample identified in the current release of HapMap. However, more mutations within the gene do exist and detailed mapping of these variants could lead to identification of a causal mutation. Following this, the mechanism of action can be learned through knock-in animal models containing the causative mutation. Additionally, these intronic and intergenic gene variants could themselves alter biological pathways through changes in expression levels.

In summary, we identified potential quantitative trait loci associated with temporal lobe volume differences at a genome-wide evidence threshold in the elderly. These candidate genes can now serve as a target of study in future large replication samples. The polymorphisms identified here may also represent risk factors for diseases with characteristic temporal lobe atrophy such as AD and its common precursor, MCI; the NMDA/glutamate pathway is also a target for anti-dementia drugs such as memantine. These associations support the theory that endophenotypes (Gottesman and Gould, 2003) will help to discover genes that influence brain structure. Ultimately studies combining imaging and genomic methods may help to provide a more mechanistic understanding of neurological and psychiatric illness.

Acknowledgments

Data used in preparing this article were obtained from the Alzheimer's Disease Neuroimaging Initiative database (www.loni.ucla.edu/ADNI). Consequently, many ADNI investigators contributed to the design and implementation of ADNI or provided data but did not participate in the analysis or writing of this report. A complete listing of ADNI investigators is available at www.loni.ucla.edu/ADNI/Collaboration/ADNI_Citation.shtml. This work was primarily funded by the ADNI (Principal Investigator: Michael Weiner; NIH grant number U01 AG024904). ADNI is funded by the National Institute of Aging, the National Institute of Biomedical Imaging and Bioengineering (NIBIB), and the Foundation for the National Institutes of Health, through generous contributions from the following companies and organizations: Pfizer Inc., Wyeth Research, Bristol-Myers Squibb, Eli Lilly and Company, GlaxoSmithKline, Merck & Co. Inc., AstraZeneca AB, Novartis Pharmaceuticals Corporation, the Alzheimer's Association, Eisai Global Clinical Development, Elan Corporation plc, Forest Laboratories, and the Institute for the Study of Aging (ISOA), with participation from the U.S. Food and Drug Administration. The grantee organization is the Northern California Institute for Research and Education, and the study is coordinated by the Alzheimer's Disease Cooperative Study at the University of California, San Diego. This study was supported by the National Institutes of Health through the NIH Roadmap for Medical Research, grant U54 RR021813 entitled Center for Computational Biology (CCB). Information on the National Centers for Biomedical Computing can be obtained from (http://nihroadmap.nih.gov/bioinformatics). Additional support was provided by grants P41 RR013642 and M01 RR000865 from the National Center for Research Resources (NCRR), a component of the National Institutes of Health (NIH). Algorithm development for this study was also funded by the NIBIB (R01 EB007813, R01 EB008281 and R01 EB008432), NICHHD (R01 HD050735), and NIA (R01 AG020098). JS was also funded by NIH/NIDA 1-T90-DA022768:02, the ARCS foundation, and the NIMH (1F31MH087061).

References

Allen Institute for Brain Science, 2009. Allen Institute Human Cortex Study. Available from: http://humancortex.alleninstitute.org. Seattle, WA.

Apostolova, L.G., Steiner, C.A., Akopyan, G.G., Dutton, R.A., Hayashi, K.M., Toga, A.W., Cummings, J.L., Thompson, P.M., 2007. Three-dimensional gray matter atrophy mapping in mild cognitive impairment and mild Alzheimer disease. Arch. Neurol. 64 (10), 1489–1495.

Bacanu, S.A., Devlin, B., Roeder, K., 2000. The power of genomic control. Am. J. Hum. Genet. 66 (6), 1933–1944.

Barrett, J.C., Fry, B., Maller, J., Daly, M.J., 2005. Haploview: analysis and visualization of LD and haplotype maps. Bioinformatics 21 (2), 263–265.

Benjamini, Y., Hochberg, Y., 1995. Controlling the False Discovery Rate — a practical and powerful approach to multiple testing. J. R. Stat. Soc. B Methodol. 57 (1), 289–300.

Bertram, L., McQueen, M.B., Mullin, K., Blacker, D., Tanzi, R.E., 2007. Systematic meta-analyses of Alzheimer disease genetic association studies: the AlzGene database. Nat. Genet. 39 (1), 17–23.

Braak, H., Braak, E., 1991. Neuropathological stageing of Alzheimer-related changes. Acta Neuropathol. 82 (4), 239–259.

Braskie, M.N., Klunder, A.D., Hayashi, K.M., Protas, H., Kepe, V., Miller, K.J., Huang, S.C., Barrio, J.R., Ercoli, L.M., Siddarth, P., Satyamurthy, N., Liu, J., Toga, A.W., Bookheimer, S.Y., Small, G.W., Thompson, P.M. in press. Plaque and tangle imaging and cognition in normal aging and Alzheimer's disease. Neurobiol. Aging. doi:10.1016/j.neurobiolaging.2008.09.012.

Brun, A., Englund, E., 1981. Regional pattern of degeneration in Alzheimer's disease: neuronal loss and histopathological grading. Histopathology 5 (5), 549–564.

Brun, C., Lepore, N., Pennec, X., Chou, Y.Y., Lee, A.D., Barysheva, M., de Zubicaray, G., Meredith, M., McMahon, K., Wright, M.J., Toga, A.W., Thompson, P.M., 2008. A tensor-based morphometry study of genetic influences on brain structure using a new fluid registration method. Int. Conf. Med. Image Comput. Comput. Assist. Interv. 11 (Pt 2), 914–921.

Brun, C.C., Lepore, N., Luders, E., Chou, Y.Y., Madsen, S.K., Toga, A.W., Thompson, P.M., 2009. Sex differences in brain structure in auditory and cingulate regions. Neuroreport 20 (10), 930–935.

Cannon, T.D., Keller, M.C., 2006. Endophenotypes in the genetic analyses of mental disorders. Annu. Rev. Clin. Psychol. 2, 267–290.

Cockrell, J.R., Folstein, M.F., 1988. Mini-Mental State Examination (MMSE). Psychopharmacol. Bull. 24 (4), 689–692.

Du, A.T., Schuff, N., Amend, D., Laakso, M.P., Hsu, Y.Y., Jagust, W.J., Yaffe, K., Kramer, J.H., Reed, B., Norman, D., Chui, H.C., Weiner, M.W., 2001. Magnetic resonance imaging of the entorhinal cortex and hippocampus in mild cognitive impairment and Alzheimer's disease. J. Neurol. Neurosurg. Psychiatry 71 (4), 441–447.

Dudbridge, F., Gusnanto, A., 2008. Estimation of significance thresholds for genome-wide association scans. Genet. Epidemiol. 32 (3), 227–234.

Farrer, L.A., Cupples, L.A., Haines, J.L., Hyman, B., Kukull, W.A., Mayeux, R., Myers, R.H., Pericak-Vance, M.A., Risch, N., van Duijn, C.M., 1997. Effects of age, sex, and

ethnicity on the association between apolipoprotein E genotype and Alzheimer disease. A meta-analysis. APOE and Alzheimer Disease Meta Analysis Consortium. JAMA 278 (16), 1349–1356.
Frazer, K.A., Ballinger, D.G., Cox, D.R., Hinds, D.A., Stuve, L.L., Gibbs, R.A., Belmont, J.W., Boudreau, A., Hardenbol, P., Leal, S.M., Pasternak, S., Wheeler, D.A., Willis, T.D., Yu, F., Yang, H., Zeng, C., Gao, Y., Hu, H., Hu, W., Li, C., Lin, W., Liu, S., Pan, H., Tang, X., Wang, J., Wang, W., Yu, J., Zhang, B., Zhang, Q., Zhao, H., Zhou, J., Gabriel, S.B., Barry, R., Blumenstiel, B., Camargo, A., Defelice, M., Faggart, M., Goyette, M., Gupta, S., Moore, J., Nguyen, H., Onofrio, R.C., Parkin, M., Roy, J., Stahl, E., Winchester, E., Ziaugra, L., Altshuler, D., Shen, Y., Yao, Z., Huang, W., Chu, X., He, Y., Jin, L., Liu, Y., Sun, W., Wang, H., Wang, Y., Xiong, X., Xu, L., Waye, M.M., Tsui, S.K., Xue, H., Wong, J.T., Galver, L.M., Fan, J.B., Gunderson, K., Murray, S.S., Oliphant, A.R., Chee, M.S., Montpetit, A., Chagnon, F., Ferretti, V., Leboeuf, M., Olivier, J.F., Phillips, M.S., Roumy, S., Sallee, C., Verner, A., Hudson, T.J., Kwok, P.Y., Cai, D., Koboldt, D.C., Miller, R.D., Pawlikowska, L., Taillon-Miller, P., Xiao, M., Tsui, L.C., Mak, W., Song, Y.Q., Tam, P.K., Nakamura, Y., Kawaguchi, T., Kitamoto, T., Morizono, T., Nagashima, A., Ohnishi, Y., Sekine, A., Tanaka, T., Tsunoda, T., Deloukas, P., Bird, C.P., Delgado, M., Dermitzakis, E.T., Gwilliam, R., Hunt, S., Morrison, J., Powell, D., Stranger, B.E., Whittaker, P., Bentley, D.R., Daly, M.J., de Bakker, P.I., Barrett, J., Chretien, Y.R., Maller, J., McCarroll, S., Patterson, N., Pe'er, I., Price, A., Purcell, S., Richter, D.J., Sabeti, P., Saxena, R., Schaffner, S.F., Sham, P.C., Varilly, P., Stein, L.D., Krishnan, L., Smith, A.V., Tello-Ruiz, M.K., Thorisson, G.A., Chakravarti, A., Chen, P.E., Cutler, D.J., Kashuk, C.S., Lin, S., Abecasis, G.R., Guan, W., Li, Y., Munro, H.M., Qin, Z.S., Thomas, D.J., McVean, G., Auton, A., Bottolo, L., Cardin, N., Eyheramendy, S., Freeman, C., Marchini, J., Myers, S., Spencer, C., Stephens, M., Donnelly, P., Cardon, L.R., Clarke, G., Evans, D.M., Morris, A.P., Weir, B.S., Mullikin, J.C., Sherry, S.T., Feolo, M., Skol, A., Zhang, H., Matsuda, I., Fukushima, Y., Macer, D.R., Suda, E., Rotimi, C.N., Adebamowo, C.A., Ajayi, I., Aniagwu, T., Marshall, P.A., Nkwodimmah, C., Royal, C.D., Leppert, M.F., Dixon, M., Peiffer, A., Qiu, R., Kent, A., Kato, K., Niikawa, N., Adewole, I.F., Knoppers, B.M., Foster, M.W., Clayton, E.W., Watkin, J., Muzny, D., Nazareth, L., Sodergren, E., Weinstock, G.M., Yakub, I., Birren, B.W., Wilson, R.K., Fulton, L.L., Rogers, J., Burton, J., Carter, N.P., Clee, C.M., Griffiths, M., Jones, M.C., McLay, K., Plumb, R.W., Ross, M.T., Sims, S.K., Willey, D.L., Chen, Z., Han, H., Kang, L., Godbout, M., Wallenburg, J.C., L'Archeveque, P., Bellemare, G., Saeki, K., An, D., Fu, H., Li, Q., Wang, Z., Wang, R., Holden, A.L., Brooks, L.D., McEwen, J.E., Guyer, M.S., Wang, V.O., Peterson, J.L., Shi, M., Spiegel, J., Sung, L.M., Zacharia, L.F., Collins, F.S., Kennedy, K., Jamieson, R., Stewart, J., 2007. A second generation human haplotype map of over 3.1 million SNPs. Nature 449 (7164), 851–861.
Freund, Y., Schapire, R.E., 1997. A decision-theoretic generalization of on-line learning and an application to boosting. J. Comput. Sys. Sci. 55 (1), 119–139.
Frisoni, G.B., Fox, N.C., Jack Jr., C.R., Scheltens, P., Thompson, P.M., 2010. The clinical use of structural MRI in Alzheimer's disease. Nat. Rev. Neurol. 6 (2), 67–77.
Genovese, C.R., Lazar, N.A., Nichols, T., 2002. Thresholding of statistical maps in functional neuroimaging using the false discovery rate. Neuroimage 15 (4), 870–878.
Gottesman, I.I., Gould, T.D., 2003. The endophenotype concept in psychiatry: etymology and strategic intentions. Am. J. Psychiatry 160 (4), 636–645.
Harold, D., Abraham, R., Hollingworth, P., Sims, R., Gerrish, A., Hamshere, M.L., Pahwa, J.S., Moskvina, V., Dowzell, K., Williams, A., Jones, N., Thomas, C., Stretton, A., Morgan, A.R., Lovestone, S., Powell, J., Proitsi, P., Lupton, M.K., Brayne, C., Rubinsztein, D.C., Gill, M., Lawlor, B., Lynch, A., Morgan, K., Brown, K.S., Passmore, P.A., Craig, D., McGuinness, B., Todd, S., Holmes, C., Mann, D., Smith, A.D., Love, S., Kehoe, P.G., Hardy, J., Mead, S., Fox, N., Rossor, M., Collinge, J., Maier, W., Jessen, F., Schurmann, B., van den Bussche, H., Heuser, I., Kornhuber, J., Wiltfang, J., Dichgans, M., Frolich, L., Hampel, H., Hull, M., Rujescu, D., Goate, A.M., Kauwe, J.S., Cruchaga, C., Nowotny, P., Morris, J.C., Mayo, K., Sleegers, K., Bettens, K., Engelborghs, S., De Deyn, P.P., Van Broeckhoven, C., Livingston, G., Bass, N.J., Gurling, H., McQuillin, A., Gwilliam, R., Deloukas, P., Al-Chalabi, A., Shaw, C.E., Tsolaki, M., Singleton, A.B., Guerreiro, R., Muhleisen, T.W., Nothen, M.M., Moebus, S., Jockel, K.H., Klopp, N., Wichmann, H.E., Carrasquillo, M.M., Pankratz, V.S., Younkin, S.G., Holmans, P.A., O'Donovan, M., Owen, M.J., Williams, J., 2009. Genome-wide association study identifies variants at CLU and PICALM associated with Alzheimer's disease. Nat. Genet. 41 (10), 1088–1093.
Hua, X., Leow, A.D., Parikshak, N., Lee, S., Chiang, M.C., Toga, A.W., Jack Jr., C.R., Weiner, M.W., Thompson, P.M., 2008. Tensor-based morphometry as a neuroimaging biomarker for Alzheimer's disease: an MRI study of 676 AD, MCI, and normal subjects. Neuroimage 43 (3), 458–469.
Jack Jr., C.R., Bernstein, M.A., Fox, N.C., Thompson, P., Alexander, G., Harvey, D., Borowski, B., Britson, P.J., J.L.W., Ward, C., Dale, A.M., Felmlee, J.P., Gunter, J.L., Hill, D.L., Killiany, R., Schuff, N., Fox-Bosetti, S., Lin, C., Studholme, C., DeCarli, C.S., Krueger, G., Ward, H.A., Metzger, G.J., Scott, K.T., Mallozzi, R., Blezek, D., Levy, J., Debbins, J.P., Fleisher, A.S., Albert, M., Green, R., Bartzokis, G., Glover, G., Mugler, J., Weiner, M.W., 2008. The Alzheimer's Disease Neuroimaging Initiative (ADNI): MRI methods. J. Magn. Reson. Imaging 27 (4), 685–691.
Jancke, L., Staiger, J.F., Schlaug, G., Huang, Y., Steinmetz, H., 1997. The relationship between corpus callosum size and forebrain volume. Cereb. Cortex 7 (1), 48–56.
Kang, H.M., Zaitlen, N.A., Wade, C.M., Kirby, A., Heckerman, D., Daly, M.J., Eskin, E., 2008. Efficient control of population structure in model organism association mapping. Genetics 178 (3), 1709–1723.
Kemp, J.A., McKernan, R.M., 2002. NMDA receptor pathways as drug targets. Nat. Neurosci. 5 (Suppl), 1039–1042.
Kent, W.J., Sugnet, C.W., Furey, T.S., Roskin, K.M., Pringle, T.H., Zahler, A.M., Haussler, D., 2002. The human genome browser at UCSC. Genome Res. 12 (6), 996–1006.
Kimura, K., Wakamatsu, A., Suzuki, Y., Ota, T., Nishikawa, T., Yamashita, R., Yamamoto, J., Sekine, M., Tsuritani, K., Wakaguri, H., Ishii, S., Sugiyama, T., Saito, K., Isono, Y., Irie, R., Kushida, N., Yoneyama, T., Otsuka, R., Kanda, K., Yokoi, T., Kondo, H., Wagatsuma, M., Murakawa, K., Ishida, S., Ishibashi, T., Takahashi-Fujii, A., Tanase, T., Nagai, K., Kikuchi, H., Nakai, K., Isogai, T., Sugano, S., 2006. Diversification of transcriptional modulation: large-scale identification and characterization of putative alternative promoters of human genes. Genome Res. 16 (1), 55–65.
Lahiri, D.K., Bye, S., Nurnberger Jr., J.I., Hodes, M.E., Crisp, M., 1992. A non-organic and non-enzymatic extraction method gives higher yields of genomic DNA from whole-blood samples than do nine other methods tested. J. Biochem. Biophys. Methods 25 (4), 193–205.
Lambert, J.C., Heath, S., Even, G., Campion, D., Sleegers, K., Hiltunen, M., Combarros, O., Zelenika, D., Bullido, M.J., Tavernier, B., Letenneur, L., Bettens, K., Berr, C., Pasquier, F., Fievet, N., Barberger-Gateau, P., Engelborghs, S., De Deyn, P., Mateo, I., Franck, A., Helisalmi, S., Porcellini, E., Hanon, O., de Pancorbo, M.M., Lendon, C., Dufouil, C., Jaillard, C., Leveillard, T., Alvarez, V., Bosco, P., Mancuso, M., Panza, F., Nacmias, B., Bossu, P., Piccardi, P., Annoni, G., Seripa, D., Galimberti, D., Hannequin, D., Licastro, F., Soininen, H., Ritchie, K., Blanche, H., Dartigues, J.F., Tzourio, C., Gut, I., Van Broeckhoven, C., Alperovitch, A., Lathrop, M., Amouyel, P., 2009. Genome-wide association study identifies variants at CLU and CR1 associated with Alzheimer's disease. Nat. Genet. 41 (10), 1094–1099.
Lamprecht, R., LeDoux, J., 2004. Structural plasticity and memory. Nat. Rev. Neurosci. 5 (1), 45–54.
Lander, E.S., Schork, N.J., 1994. Genetic dissection of complex traits. Science 265 (5181), 2037–2048.
Leow, A., Huang, S.C., Geng, A., Becker, J., Davis, S., Toga, A., Thompson, P., 2005. Inverse consistent mapping in 3D deformable image registration: its construction and statistical properties. Inf. Process. Med. Imaging 19, 493–503.
Maher, B., 2008. Personal genomes: the case of the missing heritability. Nature 456 (7218), 18–21.
Mazziotta, J., Toga, A., Evans, A., Fox, P., Lancaster, J., Zilles, K., Woods, R., Paus, T., Simpson, G., Pike, B., Holmes, C., Collins, L., Thompson, P., MacDonald, D., Iacoboni, M., Schormann, T., Amunts, K., Palomero-Gallagher, N., Geyer, S., Parsons, L., Narr, K., Kabani, N., Le Goualher, G., Boomsma, D., Cannon, T., Kawashima, R., Mazoyer, B., 2001. A probabilistic atlas and reference system for the human brain: International Consortium for Brain Mapping (ICBM). Philos. Trans. R. Soc. Lond. B Biol. Sci. 356 (1412), 1293–1322.
McCarthy, M.I., Abecasis, G.R., Cardon, L.R., Goldstein, D.B., Little, J., Ioannidis, J.P., Hirschhorn, J.N., 2008. Genome-wide association studies for complex traits: consensus, uncertainty and challenges. Nat. Rev. Genet. 9 (5), 356–369.
McKhann, G., Drachman, D., Folstein, M., Katzman, R., Price, D., Stadlan, E.M., 1984. Clinical diagnosis of Alzheimer's disease: report of the NINCDS-ADRDA Work Group under the auspices of Department of Health and Human Services Task Force on Alzheimer's Disease. Neurology 34 (7), 939–944.
Morra, J.H., Tu, Z., Apostolova, L.G., Green, A.E., Avedissian, C., Madsen, S.K., Parikshak, N., Hua, X., Toga, A.W., Jack Jr., C.R., Weiner, M.W., Thompson, P.M., 2008. Validation of a fully automated 3D hippocampal segmentation method using subjects with Alzheimer's disease mild cognitive impairment, and elderly controls. Neuroimage 43 (1), 59–68.
Morra, J.H., Tu, Z., Apostolova, L.G., Green, A.E., Avedissian, C., Madsen, S.K., Parikshak, N., Hua, X., Toga, A.W., Jack Jr., C.R., Schuff, N., Weiner, M.W., Thompson, P.M., 2009. Automated 3D mapping of hippocampal atrophy and its clinical correlates in 400 subjects with Alzheimer's disease, mild cognitive impairment, and elderly controls. Hum. Brain Mapp. 30 (9), 2766–2788.
Morris, J.C., 1993. The Clinical Dementia Rating (CDR): current version and scoring rules. Neurology 43 (11), 2412–2414.
Neitzel, H., 1986. A routine method for the establishment of permanent growing lymphoblastoid cell lines. Hum. Genet. 73 (4), 320–326.
Paling, S.M., Williams, E.D., Barber, R., Burton, E.J., Crum, W.R., Fox, N.C., O'Brien, J.T., 2004. The application of serial MRI analysis techniques to the study of cerebral atrophy in late-onset dementia. Med. Image Anal. 8 (1), 69–79.
Papassotiropoulos, A., Stephan, D.A., Huentelman, M.J., Hoerndli, F.J., Craig, D.W., Pearson, J.V., Huynh, K.D., Brunner, F., Corneveaux, J., Osborne, D., Wollmer, M.A., Aerni, A., Coluccia, D., Hanggi, J., Mondadori, C.R., Buchmann, A., Reiman, E.M., Caselli, R.J., Henke, K., de Quervain, D.J., 2006. Common Kibra alleles are associated with human memory performance. Science 314 (5798), 475–478.
Parsons, C.G., Stoffler, A., Danysz, W., 2007. Memantine: a NMDA receptor antagonist that improves memory by restoration of homeostasis in the glutamatergic system—too little activation is bad, too much is even worse. Neuropharmacology 53 (6), 699–723.
Peper, J.S., Brouwer, R.M., Boomsma, D.I., Kahn, R.S., Hulshoff Pol, H.E., 2007. Genetic influences on human brain structure: a review of brain imaging studies in twins. Hum. Brain Mapp. 28 (6), 464–473.
Petersen, R.C., 2000. Aging, mild cognitive impairment, and Alzheimer's disease. Neurol. Clin. 18 (4), 789–806.
Petersen, R.C., Smith, G.E., Waring, S.C., Ivnik, R.J., Tangalos, E.G., Kokmen, E., 1999. Mild cognitive impairment: clinical characterization and outcome. Arch. Neurol. 56 (3), 303–308.
Potkin, S.G., Turner, J.A., Fallon, J.A., Lakatos, A., Keator, D.B., Guffanti, G., Macciardi, F., 2009a. Gene discovery through imaging genetics: identification of two novel genes associated with schizophrenia. Mol. Psychiatry 14 (4), 416–428.
Potkin, S.G., Turner, J.A., Guffanti, G., Lakatos, A., Torri, F., Keator, D.B., Macciardi, F., 2009b. Genome-wide strategies for discovering genetic influences on cognition and cognitive disorders: methodological considerations. Cognit. Neuropsychiatry 14 (4–5), 391–418.
Purcell, S., Neale, B., Todd-Brown, K., Thomas, L., Ferreira, M.A., Bender, D., Maller, J., Sklar, P., de Bakker, P.I., Daly, M.J., Sham, P.C., 2007. PLINK: a tool set for whole-genome association and population-based linkage analyses. Am. J. Hum. Genet. 81 (3), 559–575.
Sabatti, C., Service, S.K., Hartikainen, A.L., Pouta, A., Ripatti, S., Brodsky, J., Jones, C.G., Zaitlen, N.A., Varilo, T., Kaakinen, M., Sovio, U., Ruokonen, A., Laitinen, J., Jakkula, E., Coin, L., Hoggart, C., Collins, A., Turunen, H., Gabriel, S., Elliot, P., McCarthy, M.I., Daly, M.J., Jarvelin, M.R., Freimer, N.B., Peltonen, L., 2009. Genome-wide association analysis of metabolic traits in a birth cohort from a founder population. Nat. Genet. 41 (1), 35–46.

Please cite this article as: Stein, J.L., et al., Genome-wide analysis reveals novel genes influencing temporal lobe structure with relevance to neurodegeneration in Alzheimer's disease, NeuroImage (2010), doi:10.1016/j.neuroimage.2010.02.068

Schito, A.M., Pizzuti, A., Di Maria, E., Schenone, A., Ratti, A., Defferrari, R., Bellone, E., Mancardi, G.L., Ajmar, F., Mandich, P., 1997. mRNA distribution in adult human brain of GRIN2B, a N-methyl-D-aspartate (NMDA) receptor subunit. Neurosci. Lett. 239 (1), 49–53.

Schwirzke, M., Gnirke, A., Bork, P., Tarin, D., Weidle, U.H., 1998. Differential gene expression in mammary carcinoma cell lines: identification of DRIM, a new gene down-regulated in metastasis. Anticancer Res. 18 (3A), 1409–1421.

Seshadri, S., DeStefano, A.L., Au, R., Massaro, J.M., Beiser, A.S., Kelly-Hayes, M., Kase, C.S., D'Agostino Sr., R.B., Decarli, C., Atwood, L.D., Wolf, P.A., 2007. Genetic correlates of brain aging on MRI and cognitive test measures: a genome-wide association and linkage analysis in the Framingham Study. BMC Med. Genet. 8 (Suppl 1), S15.

Small, G.W., Siddarth, P., Burggren, A.C., Kepe, V., Ercoli, L.M., Miller, K.J., Lavretsky, H., Thompson, P.M., Cole, G.M., Huang, S.C., Phelps, M.E., Bookheimer, S.Y., Barrio, J.R., 2009. Influence of cognitive status, age, and APOE-4 genetic risk on brain FDDNP positron-emission tomography imaging in persons without dementia. Arch. Gen. Psychiatry 66 (1), 81–87.

Tang, Y.P., Shimizu, E., Dube, G.R., Rampon, C., Kerchner, G.A., Zhuo, M., Liu, G., Tsien, J.Z., 1999. Genetic enhancement of learning and memory in mice. Nature 401 (6748), 63–69.

Tanzi, R.E., 1999. A genetic dichotomy model for the inheritance of Alzheimer's disease and common age-related disorders. J. Clin. Invest. 104 (9), 1175–1179.

Thompson, P.M., Martin, N.G., 2010. The ENIGMA Network. URL: http://enigma.loni.ucla.edu.

Thompson, P.M., Narr, K.L., Blanton, R.E., Toga, A.W., 2002. Mapping structural alterations of the corpus callosum during brain development and degeneration. In: Zaidel, E., Iacoboni, M. (Eds.), The Parallel Brain: the Cognitive Neuroscience of the Corpus Callosum. MIT Press.

Thompson, P.M., Hayashi, K.M., de Zubicaray, G., Janke, A.L., Rose, S.E., Semple, J., Herman, D., Hong, M.S., Dittmer, S.S., Doddrell, D.M., Toga, A.W., 2003. Dynamics of gray matter loss in Alzheimer's disease. J. Neurosci. 23 (3), 994–1005.

Thompson, P.M., Hayashi, K.M., Dutton, R.A., Chiang, M.C., Leow, A.D., Sowell, E.R., De Zubicaray, G., Becker, J.T., Lopez, O.L., Aizenstein, H.J., Toga, A.W., 2007. Tracking Alzheimer's disease. Ann. N. Y. Acad. Sci. 1097, 183–214.

Toro, R., Perron, M., Pike, B., Richer, L., Veillette, S., Pausova, Z., Paus, T., 2008. Brain size and folding of the human cerebral cortex. Cereb. Cortex 18 (10), 2352–2357.

Ushkaryov, Y.A., Petrenko, A.G., Geppert, M., Sudhof, T.C., 1992. Neurexins: synaptic cell surface proteins related to the alpha-latrotoxin receptor and laminin. Science 257 (5066), 50–56.

Waring, S.C., Rosenberg, R.N., 2008. Genome-wide association studies in Alzheimer disease. Arch. Neurol. 65 (3), 329–334.

Wellcome Trust Case Control Consortium, 2007. Genome-wide association study of 14,000 cases of seven common diseases and 3,000 shared controls. Nature 447 (7145), 661–678.

Yashiro, K., Philpot, B.D., 2008. Regulation of NMDA receptor subunit expression and its implications for LTD, LTP, and metaplasticity. Neuropharmacology 55 (7), 1081–1094.

Glossary

TBM: tensor-based morphometry
MDT: minimal deformation template
AD: Alzheimer's disease
MCI: mild cognitive impairment
ADNI: Alzheimer's Disease Neuroimaging Initiative
SNP: single nucleotide polymorphisms
NMDA receptor: *N*-methyl-D-aspartate glutamate receptor
LD: linkage disequilibrium
OR: odds ratio
FDR: false discovery rate
EST: expressed sequence tag

Please cite this article as: Stein, J.L., et al., Genome-wide analysis reveals novel genes influencing temporal lobe structure with relevance to neurodegeneration in Alzheimer's disease, NeuroImage (2010), doi:10.1016/j.neuroimage.2010.02.068